submitted to *Int. J. Mass Spectrom.*

Role of Methylation on the Thermochemistry of Alkali Metal Cation Complexes of Amino Acids: N-Methyl Proline [a]

A. Mookherjee and P. B. Armentrout*

Department of Chemistry, University of Utah, Salt Lake City, UT 84112, United States

ABSTRACT: Quantitative thermodynamic information is obtained from the study of the gas-phase interactions of the alkali metal cation complexes of N-methyl proline (NMP) with Xe using a guided ion beam tandem mass spectrometer (GIBMS). Absolute bond dissociation energies (BDEs) of M^+ = Li^+, Na^+, K^+, and Rb^+ to NMP are determined experimentally from threshold collision-induced dissociation (TCID) measurements of the M^+(NMP) complexes. Analysis of their kinetic energy cross sections provide the 0 K bond enthalpies after accounting for unimolecular decay rates, internal energy of reactant ions, and multiple ion-molecule collisions. Quantum chemical calculations of the M^+(NMP) BDEs are found to be in good agreement with the experimental values, establishing that the zwitterionic form is the lowest energy structure for all the metal ion complexes. Compared to M^+(Pro) BDEs, the metal binding in these zwitterions is slightly enhanced by the CH_3 group on the ring nitrogen, presumably a result of an inductive effect and its higher polarizability. More profound consequences of the methyl group emerge in the charge-solvated conformers calculated for M^+(NMP) where it directs multiple conformations of the pyrrolidine ring. This is unlike the ring puckering phenomenon seen in M^+(Pro) complexes, where fewer conformations are found, apparently because inversion at the nitrogen center is more facile.

Key words: bond dissociation energies, collision-induced dissociation, energy-resolved mass spectrometry, methylation, proline

[a] In honor of Keith Jennings and Jim Scrivens on the occasion of their notable birthdays.

* Corresponding author. Tel.: +1 801 581 7885; fax: +1 801 581 8433.

E-mail address: armentrout@chem.utah.edu (P.B. Armentrout).

UU IR Author Manuscript

1. Introduction

Amino acids exist as zwitterionic structures in solution phase. In the gas phase, these charge separated species lack the stabilization of the solvation shell, but can be stabilized by metal cations. By studying these systems in the absence of solvent media, the native interaction of a metal cation with an amino acid can be appraised. Previous work has determined the absolute bond dissociation energies (BDEs) of the alkali metal cation complexes of many amino acids: glycine, proline, serine, threonine, asparagine, aspartic acid, glutamine, glutamic acid, methionine, cysteine, phenylalanine, tyrosine, and tryptophan, using threshold collision-induced dissociation (TCID) [1-11], in which the energy onset for fragmentation of thermalized complexes is carefully measured [12-14]. The objective of this work is to help develop a "thermodynamic vocabulary" [15] of pairwise binding energies of the metal ions to amino acids, which can be used to deduce the relative contributions of interactions that stabilize the amino acids and to better understand the interactions of metal ions in more complex biological systems.

N-methyl proline (NMP) is a modification of the proline molecule in which the hydrogen on the secondary amine group in proline (Pro) is replaced by a methyl (CH_3) group. Unlike proline, NMP is rarely observed in nature, although it has been isolated from several angiosperm species [16], where it was reported to function in abiotic stress resistance. It was also documented [17] as a part of a chemotactic peptide obtained from the alkali-degradation of the cornea from the eye. With the help of protein sequencing and mass spectrometry, NMP-Gly-Pro was identified as one of the chemoattractants released on alkali degradation. The chemoattractant was believed to play a major role in the early neutrophil response of alkali degraded corneas.

Using TCID, proline complexes with $M^+ = Li^+$, Na^+, K^+, and Rb^+ have been studied previously [2,6]. By comparison with quantum chemical calculations, these complexes were identified as having a zwitterionic structure in which the metal binds to the oxygen atoms of the carboxylate group. Infrared multiple photon dissociation (IRMPD) action spectroscopy using free electron lasers coupled with quantum chemical calculations have also been used to establish the ground state zwitterionic character of Na^+(Pro) by Kapota et al. [18] and of K^+(Pro) by Drayβ

et al. [19]. IRMPD studies have also been done for K^+(NMP) by Drayβ et al. [20,21], again identifying a zwitterionic structure for this complex, and comparing the results to those for potassiated Pro, NMP-methylester, and N-methyl alanine. In conjunction with this work, a preliminary TCID study of this complex was also conducted [22].

The current work investigates the non-covalent interactions of NMP with alkali metal cations, $M^+ = Li^+$, Na^+, K^+, and Rb^+. Building upon previous work done on M^+(Pro) [2,6], this study helps better understand differences in the dissociation dynamics induced by the tertiary nitrogen. To complement the experiments, quantum chemical calculations are performed to determine the low-energy conformers of these complexes and the bare ligand along with their molecular constants (rotational constants and vibrational frequencies) needed for data analysis. Further calculations were done at several levels of theory using the optimized geometries to compute BDEs for comparison with the experimental results. These comparisons allow the geometry of the ground state complexes to be positively identified as zwitterionic for all four alkali metal cations.

2. Experimental and computational section

2.1 General procedures

The instrument used to measure the cross sections for CID of the metal-ligand complexes of NMP is a guided ion beam tandem mass spectrometer (GIBMS), which has been described in detail previously [23,24]. The metal-ligand complex ions were made in an electrospray ionization (ESI) source described elsewhere [25]. In brief, solutions of 10^{-3} M NMP and 10^{-3} M LiCl, NaOH, KCl, or RbCl were made in a 50:50 HPLC H_2O/MeOH solution. NMP was provided by the Schäfer group [22], whereas all other materials were purchased from Sigma Aldrich. These solutions were sprayed at a rate of 0.04 mL/hr from a stainless steel needle biased at a voltage of ~ 2 kV. Ions enter the vacuum through a capillary, which is maintained at 80 °C, and are collected by a radio-frequency (rf) ion-funnel [26]. They then enter an rf hexapole ion guide, where the ions undergo multiple collisions (> 10^4) with background gases and become

UU IR Author Manuscript

thermalized. Ions produced by this source are assumed to have their internal energy well described by a Maxwell-Boltzmann distribution of rovibrational states at 300 K, as documented previously [4,5,9,25,27,28]. These metal-ligand complexes are extracted from the source and mass-selected by a magnetic momentum mass analyzer. The ion beam is then decelerated to a well-defined variable kinetic energy and focused into an rf octopole ion guide that traps the ions radially, reducing losses of the reactant and product ion species from scattering [23,29,30]. The octopole guides the ions through a gas cell containing the inert gas xenon at low enough pressures to ensure single collision conditions. Xenon is chosen as the collision gas for reasons described previously [31,32]. After collision with xenon, remaining reactant and product ions move toward the exit end of the octopole ion guide where they are focused into a quadrupole mass filter for mass analysis. The ions are then detected by a high voltage dynode and scintillation ion detector [33], which is interfaced with fast-counting electronics. Ion intensities, measured as a function of the ion kinetic energy, are converted to absolute cross sections as described previously [23]. Uncertainties in relative cross sections are about ± 5% whereas those for absolute cross sections are about ± 20%. The ion kinetic energy distribution and the absolute zero of the energy scale is measured using the octopole ion guide, which functions as an efficient retarding energy analyzer [23]. The energy distribution is Gaussian, having a typical FWHM of 0.15 – 0.20 eV (lab), and the absolute energy scale has an uncertainty of 0.05 eV (lab). Ion kinetic energies in the laboratory (lab) frame are converted to the center-of-mass (CM) frame using the formula $E_{CM} = E_{lab}\, m/(m+M)$, where M and m are the masses of the ionic and neutral species, respectively. Energies reported below are in the CM frame unless otherwise noted.

2.2. Data analysis

The threshold regions of the CID reaction cross sections are modeled using Eq. (1),

$$\sigma(E) = \sigma_0 \sum g_i (E + E_i - E_0)^n / E \qquad (1)$$

where σ_0 is an adjustable energy-independent parameter, n is an adjustable parameter that describes the efficiency of energy deposition during a collision [24], E is the relative kinetic energy of the reactants, and E_0 is the threshold for collision-induced dissociation at 0 K. The summation is taken over the rovibrational states of the reactant ions, i, where E_i represents the internal energy of each state with fractional population g_i, where $\sum g_i = 1$. Thus $E + E_i$ is the total energy available to the colliding reactants. Vibrational frequencies and rotational constants for the calculation of E_i and g_i are obtained from quantum chemical calculations discussed in the next section. The Beyer-Swinehart-Stein-Rabinovitch algorithm [34,35] is used to evaluate the density of the rovibrational states and the fractional populations g_i are calculated for a Maxwell-Boltzmann distribution at 300 K.

Several systematic issues complicate the interpretation of TCID data and must be addressed in order to obtain accurate thermodynamic data. Because the number of internal modes available to randomize the energy increases with the size of the molecule, large molecules may not dissociate efficiently during the experimental time available, $\tau \sim 5 \times 10^{-4}$ s. This results in a kinetic shift such that products are not seen until energies higher than the true threshold. These kinetic shifts are estimated by complementing the CID model of Eq. (1) with a statistically calculated probability of dissociation, leading to Eq. (2) [36].

$$\sigma(E) = \frac{n\sigma_0}{E} \sum g_i \int_{E_0 - E_i}^{E} P_D(\varepsilon)(E - \varepsilon)^{n-1} \mathrm{d}\varepsilon \qquad (2)$$

For CID reactions, the probability of dissociation, $P_D(\varepsilon)$, is given by 1 - exp[-$k(E^*)\tau$], where $k(E^*)$ is the unimolecular rate constant of dissociation, $E^* = \varepsilon + E_i$ is the energy of the energized molecule (EM) after the collision, ε is the energy transferred from translation to internal energy of the reactant complex during collision, and the reaction occurs only when $E^* \geq E_0$. Eq. (2) reduces to Eq. (1) when $k(E^*)$ is much faster than the experimental time available for dissociation. The unimolecular dissociation rate constant, $k(E^*)$, is defined by Rice-Ramsperger-Kassel-Marcus (RRKM) theory [37,38], as shown in Eq. (3).

UU IR Author Manuscript

$$k(E^*) = \frac{dN_{vr}^{\dagger}(E^* - E_0)}{h\rho_{vr}(E^*)} \quad (3)$$

Here d is the reaction degeneracy, h is Planck's constant, $N_{vr}^{\dagger}(E^* - E_0)$ is the sum of rovibrational states of the transition state (TS) at the energy $E^* - E_0$, and $\rho_{vr}(E^*)$ is the density of rovibrational states of the energized molecule (EM) at the available energy E^*. Evaluation of Eq. (3) requires vibrational frequencies and rotational constants of the TS and EM, which are taken from the quantum chemical calculations. The M^+(NMP) complexes dissociate to give M^+ and NMP via loose TSs that are located at the centrifugal barrier appropriate for an ion-induced dipole potential, as the dissociation involves simple heterolytic bond cleavage [36,39]. The TS is product-like with the incipient fragments able to rotate freely, which is the underlying assumption of the phase space limit (PSL) [36,40,41]. In this limit, the TS frequencies are those of the dissociated products with the transitional frequencies for NMP loss treated as rotors. The adiabatic 2-D rotational energy is treated using a statistical distribution with a summation over the possible values of the rotational quantum number.

Eqs. (1) and (2) describe models for cross sections representing products that are formed as a result of a single collision event. Multiple ion-neutral collisions can deposit more energy at the same laboratory ion energy resulting in a lowering of the observed reaction threshold. In order to impose rigorous single collision conditions, data are collected at three different pressures of xenon: ~ 0.05, 0.10, and 0.20 mTorr, and then the cross sections are extrapolated to zero pressure [42]. Such zero-pressure extrapolated cross sections are analyzed to extract thresholds.

Before making a comparison with the experimental data, Eq. (1) or (2) is convoluted over the kinetic energy distributions of the reactant ion and thermal energy distribution of the neutral gas, as previously detailed [23,43,44]. A nonlinear least-squares method is used to optimize the values of σ_0, n, and E_0. Uncertainties in these parameters are estimated from the range of values that are determined from different data sets and include variations in vibrational frequencies (± 10%), in the parameter n (± 10%), in τ by a factor of 2, and the uncertainty in the absolute energy scale of 0.05 eV (lab). The final 0 K bond energies are obtained from the optimized thresholds

UU IR Author Manuscript

on the basis of two assumptions. First, there are no activation barriers in excess of the endothermicity for the loss of the ligand. This assumption is generally true for ion-molecule reactions and for heterolytic bond cleavages, which is the case here [39]. Second, the measured threshold corresponds to the dissociation of the ground state reactant to the ground state product ion and neutral ligand. Given the available time, ~ 5×10^{-4} s, the dissociating complex has sufficient time to explore phase space, thereby allowing rearrangement to the ground state conformation of the products upon dissociation.

2.3. Computational details

Model structures, vibrational frequencies, and energetics were obtained for the neutral ligand and the metalated complexes using Gaussian09 [45]. The metal complex, M^+(NMP), and the neutral ligand, NMP, have several geometric conformers. Different geometries within ~ 110 kJ/mol of the lowest energy structure of K^+(NMP) and NMP were obtained previously at the B3LYP/6-311++G(2d,2p) level [22]. They served as starting structures for geometry optimizations at the B3LYP/6-311+G(d,p) level for Li^+(NMP), Na^+(NMP), and K^+(NMP) and at the B3LYP/def2-TZVP level for Rb^+(NMP). The def2-TZVP basis set provides a size consistent basis set on all atoms at the triple zeta level including polarization functions [46] and makes use of a small core effective core potential (ECP) on rubidium [47]. Experimental and theoretical BDEs of Rb^+(AA), AA = glycine, proline, serine, threonine, and cysteine [6,7], have been shown to agree well when using the def2-TZVP basis set. Geometries of Na^+(NMP) and K^+(NMP) were also optimized at the B3LYP/def2-TZVP level for comparison with the B3LYP/6-311+G(d,p) geometries. Rotational constants and the vibrational frequencies were calculated at the B3LYP/6-311+G(d,p) level for Li^+ (NMP), at the B3LYP/6-311+G(d,p) and B3LYP/def2-TZVP levels for Na^+(NMP) and K^+(NMP), and at the B3LYP/def2-TZVP level for Rb^+(NMP). When used in RRKM calculations, the frequencies were scaled by a factor of 0.9804 [48]. The vibrational frequencies and rotational constants of the lowest energy complex for all four metal complexes and the neutral ligand are listed in Tables 1S and 2S of the supporting information. Conformers

obtained from the geometry optimizations were used to calculate single point energies at the B3LYP, B3P86, and MP2(full) levels using the 6-311+G(2d,2p) for Li^+(NMP), 6-311+G(2d,2p) and def2-TZVP basis sets for Na^+(NMP) and K^+(NMP), and def2-TZVP basis set for Rb^+(NMP). Single point energy calculations were also performed using the def2-TZVPP basis set for the ground state conformers of Li^+(NMP), Na^+(NMP), K^+(NMP), and Rb^+(NMP). The def2-TZVP and def2-TZVPP basis sets for $M^+ = Na^+$, K^+, and Rb^+ were obtained from the EMSL basis set exchange library [49,50]. Zero-point vibrational energy (ZPE) corrections were determined using the scaled vibrational frequencies calculated as described above. Basis set superposition errors (BSSE) were estimated for the BDEs using the full counterpoise (cp) method [51]. Counterpoise corrections were found to be 5 – 9 kJ/mol at the MP2(full) level and 1 – 3 kJ/mol for B3LYP and B3P86 single point energies. This is consistent with previous results obtained using alkali metal cation systems that cp corrections for density functional theory (DFT) calculations are generally small [2,7,9]. Feller et al. suggest that the theoretical MP2(full) energies calculated without BSSE corrections may be closer to experimental values than those calculated with cp corrections [52,53]. Because the most accurate MP2 values may fall between those with and without the BSSE corrections, both are reported below.

The smaller ion size of lithium leads to shorter M^+–NMP bond distances, with greater electronic distortion of the ligand upon complexation. These shorter metal-ligand bond lengths can result in repulsive interactions between the closed-shell core electrons on Li^+ and the closed-shell ligand [54]. This effect can be taken into consideration by letting the core electrons on the metal cation polarize away from the ligand and correlate with the ligand electrons, but standard basis sets do not include such correlation functions on Li^+. Therefore calculations were also performed using the correlation consistent polarized core/valence basis sets (cc-pCVXZ, X = D and T here) developed by Dunning to describe Li^+ [55,56]. Hence, the structures of Li^+(NMP) were optimized at B3LYP and MP2(full) levels using the cc-pCVDZ basis set for Li^+ and the cc-pVDZ basis set on other atoms, referred to as cc-pVDZ(Li-C) below. Single point energies were calculated at B3LYP, B3P86, and MP2(full) levels using the cc-pCVTZ basis set on Li^+ and the

UU IR Author Manuscript

aug-cc-pVTZ basis set on other atoms, referred to as aug-cc-pVTZ(Li-C) below. It may be inappropriate to apply counterpoise corrections to the single point energy calculations at the MP2(full) level as they have been shown to reduce the accuracy of the computational results [54].

3. Results

3.1. Theoretical results for NMP

Three types of conformations of the NMP ligand were examined, each with different intramolecular hydrogen bonding. These three motifs (N1, N2, and N3) are similar to those observed in Pro [2], where the nomenclature used here was developed. The α carbon is labeled C1, and the remaining ring carbons are labeled C2 through C4, moving toward the amine group. The five-membered ring of NMP develops a pucker in the ring with one atom lying out of the plane relative to the other four. Here, the four atoms in the ring with a dihedral angle closest to zero are considered "planar". The "out-of-plane" atom is designated as "up" if it lies on the same side of the ring as the carboxylate or carboxylic acid group and "down" if on the opposite side. This differs somewhat from the nomenclature adopted for Pro where all structures could be described as C3-up or C3-down [2,6].

Ten possible structures for each N1 – N3 motif can be envisioned as each of the five atoms in the five-membered ring can be in "up" or "down" puckered positions relative to the other four atoms. All possible conformations of NMP were optimized at the B3LYP/6-311+G(d,p) level, with results showing that all conformations collapse to one of the nine structures in Table 1 and Fig. 1. Calculations using the def2-TZVP basis set give very similar geometries and relative energies, within 2 kJ/mol in all cases (Table 1).

As found previously [22], the N2 C3-up conformer is the ground state conformation and is stabilized by a strong N···HO hydrogen bond of 1.89 Å. Similarly, Moision et al. report the N2 C3-up form of proline, having a N···HO hydrogen bond of 1.86 Å, as the most stable structure of proline [2]. Thus, the methyl group on the ring amine nitrogen has little affect on the ground state of the molecule. The next higher energy conformer is the N2 C2-up structure, which differs

from the C3-up structure only in the position of the carbon that is puckered. (In proline, this geometry is equivalent to the C3-down structure [2].) All three levels of theory show that the C3-up conformation is favored over the C2-up conformation by ~ 6 kJ/mol (Table 1). This destabilization appears to be primarily the result of a slightly longer N···HO bond, now 1.94 Å.

Six conformers, which have energies in the range of 9 – 18 kJ/mol, replace the N···HO hydrogen bond of N2 by a weaker OH···OC interaction (2.28 – 2.29 Å) for both N3 and N1 binding motifs. Three different ring puckering positions for each motif were observed: C3-up, C1-up, and N-up, as shown in Table 1 and Fig. 1. Because the N3 and N1 forms differ only in the orientation of the carboxylic acid groups relative to the ring, they have similar energies, within 1 – 3 kJ/mol of one another for all three ring puckering positions. For proline, Moision et al. also report the N1 and N3 forms, which both have C3-up and C4-up conformers. The N1 forms lie within 5 – 9 kJ/mol of the C3-up N2 ground state of Pro, whereas the N3 forms lie 12 – 17 kJ/mol above the ground state [2].

The highest energy conformation located is a N2 N-up conformer, higher than the ground state by 30 – 37 kJ/mol. This is partially because it has a much longer N···HO bond, 2.24 Å, than the other N2 conformers. In addition, the ∠(O)CC1NC(H_3) dihedral angle is 56° in this conformer compared with -100° in N2 C3-up and -89° in N2 C2-up. Thus, the methyl group is gauche to the carboxylic acid group, leading to a repulsive interaction.

3.2. Theoretical results for M^+(NMP)

Low and high-energy conformations of Na^+(NMP) complexes are shown in Fig. 2 and are representative of all metal cation complexes, with relative energies listed in Table 2. The already established nomenclature for metal-ligand complexes [1,8,57-59] is used in the current work. The notation in brackets denotes the site of coordination of the metal ion to the ligand, followed by a description of the ring puckering position and the ∠HOCC dihedral angle wherever necessary to distinguish similar conformers. The dihedral angle is designated c for cis when the angle is less than 50°, and t for trans when the angle is greater than 135°. Some geometric details

UU IR Author Manuscript

of the complexes are included in Table S3 of the supporting information. Calculations using the def2-TZVP basis set for Na^+(NMP) and K^+(NMP) give very similar geometries (Table S3) and relative energies within 5 kJ/mol in all cases (Table 2).

At all levels of theory, the ground state structure for Li^+(NMP), Na^+(NMP), K^+(NMP), and Rb^+(NMP) is the [CO_2^-] C3-up conformer, a bidentate structure in which the metal ion binds to both carboxylate oxygens, as previously found for K^+(NMP) [22]. The C3-down variant of this structure is only 3 – 6 kJ/mol higher in energy for all four metal-ligand complexes. Strong intramolecular hydrogen bonds drive the strongly preferred ring puckered locations of the M^+(NMP) complexes. As the C3-up conformer changes to a C3-down conformer, calculations show that the ∠C3C2C1C(O) dihedral angles change from ~ –90° to ~ –143°, which leads to the elongation of the NH···OC hydrogen bond by an average of 0.048 ± 0.004 Å. The [CO_2^-] C3-up structure was also found to be the ground state structure for alkali metal cation complexes of proline [2,6]. This shows that the ground states of M^+(Pro) and M^+(NMP) are driven primarily by the high basicity of the secondary and tertiary nitrogen combined with the NH···OC hydrogen bond. The [CO_2^-] C3-down structure was also found for the M^+(Pro) complexes and again was higher in energy than the [CO_2^-] C3-up conformer by 3 – 6 kJ/mol, for similar reasons as elucidated here [2,6].

Two additional conformers, N-up and C1-up, also show [CO_2^-] coordination in all four metal complexes, but in both cases, the proton on N now lies on the opposite side of the ring compared to the carboxylate groups. As a result, the NH proton cannot interact strongly with the carboxylate oxygens and there are steric interactions between the CO_2^- and CH_3 groups. Thus, the N-up and C1-up structures lie 30 – 42 kJ/mol above the ground state conformer of each complex.

Another unique binding pattern of the metal ion observed in the M^+(NMP) systems is the [COOH] structure, the charge-solvated variant of [CO_2^-] in which the proton from the nitrogen is transferred to the OH of the carboxylic group. The metal remains coordinated with both oxygens of the carboxylic acid group. There are three variants of this kind of structure, C3-up, C3-down,

UU IR Author Manuscript

and N-up, where the latter is much higher is energy. The [COOH] C3-down conformer in the metal cation complexes is higher than [COOH] C3-up by 6 – 8 kJ/mol, comparable to the difference found for the [CO_2^-] analogues. Calculations show that the C3 conformers are higher in energy than the [CO_2^-] analogues by 15 – 39 kJ/mol for Na^+(NMP), K^+(NMP), and Rb^+(NMP), but collapse to the zwitterion for Li^+(NMP) and for Na^+(NMP) when the def2-TZVP basis set is used. More electron density from the oxygens of CO_2^- is required to solvate the strongly bound Li^+ relative to the other three alkali metal ions. This lessens the electron density available for the formation of the N···HO hydrogen bond, and as a result there is no barrier to transferring the proton to the nitrogen forming a zwitterion in the case of Li^+(NMP). Similar [COOH] C3-up and [COOH] C3-down conformers were also observed for M^+(Pro) where M^+ = Na^+, K^+, and Rb^+ [2,6]. As also observed here, the [COOH] C3-up and [COOH] C3-down conformers of Li^+(Pro) collapse into the respective [CO_2^-] structures; however, a stable [CO] C3-up structure was located for Li^+(Pro).

A high-energy variant of the [COOH] structure is also found in all four metal cation M^+(NMP) complexes. The [COOH] N-up structures lie higher than the [CO_2^-] N-up analogues by 27 – 82 kJ/mol. The two structures differ primarily in the position of the hydrogen, but this change forces one of the M^+-OC bond distances to increase appreciably, by 0.12, 0.16, 0.29, and 0.44 Å for Li^+, Na^+, K^+, and Rb^+, respectively, leading to the higher energy.

Four variations of the [N, CO] structure, in which the metal binds to the nitrogen and carbonyl oxygen in a charge-solvated complex were located with C4-down and N-up puckered positions. For each of these, the orientation of the OH hydrogen, ∠HOCC, can be trans, in which case it can interact with the carbonyl oxygen, or it can be cis, in which case the stabilization of the OH···OC interaction is lost. The [N, CO] C4-down, t structure is higher in energy than the [CO_2^-] C3-up ground state by 24 – 39 kJ/mol and the [N, CO] C4-down, c structure is higher still by another 18 – 21 kJ/mol. The difference in energies between the N-up and C4-down structures results from the position of the methyl groups in these conformers, which is gauche to the carboxylate group in the N-up structures. The methyl groups are perched

UU IR Author Manuscript

directly over the ring in the N-up structures, creating an overall constrained structure as shown in Fig. 2. As the pucker changes from C4-down to N-up, the M^+─N bond distances decrease slightly (by 0.01 – 0.09 Å) but the M^+─OC bond distances increase by 0.04 – 0.06 Å. Thus, the N-up, t structures are higher in energy than the C4-down, t by 20 – 37 kJ/mol, with the N-up, c structures another 10 – 21 kJ/mol higher in energy. [N, CO] coordinated structures were also found for the M^+(Pro) complexes and correspond to the C4-down and N-up structures in M^+(NMP) (but were called C3-up and C3-down originally). These structures are 13 – 26 and 9 – 42 kJ/mol, respectively, higher than the corresponding zwitterions [2,6].

Two other kinds of metal ion binding patterns seen in the M^+(NMP) complexes are [N, OH] and [CO], both of which are very high in energy compared to the ground states, Table 2. In the [N, OH] bidentate structure, the metal binds to the amine nitrogen and the hydroxyl oxygen of COOH to form a charge-solvated complex that lies 62 – 77 kJ/mol above the [CO_2^-] C3-up ground state. Furthermore, these structures lie above their [N, CO] C4-down, t analogues (see Fig. 2) by 24 – 45 kJ/mol because the carbonyl is a better metal cation binding site than the hydroxyl group [1,8]. The M^+(NMP) [N, OH] complexes have similar structures for all four metals but the most planar ring atoms change such that Li^+(NMP) is C4-down, but the other three alkali metal complexes are N-up. For comparison, the [N, OH] conformer for M^+(Pro), which was not examined in previous work, was calculated here. We find it is puckered C2-down in Li^+(Pro), C4-down in Na^+(Pro), and N-up for both K^+(Pro) and Rb^+(Pro). The M^+(Pro) [N, OH] conformers are 52 – 68 kJ/mol higher in energy than the respective ground states and another 19 – 47 kJ/mol higher than the [N, CO] conformers, respectively.

In the [CO] structure, the metal binds only to the carbonyl oxygen of COOH in a charge-solvated complex with a C1-up ring pucker and the methyl group is gauche with the carboxylic acid group. The hydroxyl group can have either a t or c orientation, where the latter is 3 – 8 kJ/mol higher in energy. The [CO] C1-up, t conformer is higher in energy than the [CO_2^-] C3-up ground state by 62 – 95 kJ/mol in the Na^+, K^+, and Rb^+ complexes, but collapses into the [N, CO] C4-down, t structure for Li^+. This transformation requires that the symmetry at the nitrogen

UU IR Author Manuscript

atom inverts (umbrella motion), which is apparently driven by the strong field induced by the small lithium cation. Moision et al. reported a [CO] structure for Li^+(Pro) C3-up that is 37 – 45 kJ/mol higher than its ground state, whereas the Na^+(Pro) and K^+(Pro) [CO] conformers collapsed to their respective [N, CO] C3-up conformers [2]. Bowman et al. reported the Rb^+(Pro) [CO] C3-up structure to be 52 – 57 kJ/mol higher than its ground state [6].

3.3. Cross sections for collision–induced dissociation

Experimental TCID cross sections were obtained for all four alkali metal cation complexes. The loss of the intact amino acid, NMP, in reaction (4) was observed for all four M^+(NMP) complexes and is the only dissociation channel for Na^+(NMP), K^+(NMP), and Rb^+(NMP).

$$M^+(NMP) + Xe \rightarrow M^+ + NMP + Xe \quad (4)$$

Fig. 3 shows zero-pressure extrapolated cross sections for these three complexes. In addition to reaction (4), Li^+(NMP) shows additional fragmentation processes at lower collision energies, mainly loss of CO + H_2O along with CO + LiOH, which are summed together in Fig. 3a. Analysis of the Li^+(NMP) data is elaborate as it requires 1) accounting for competition between the low-energy fragmentation channels and reaction (4), and 2) the calculation of tight transition states that lead to the low-energy channels. Because of the complexity of these fragmentation reactions, these results and their detailed threshold analysis will be provided in a subsequent publication [60].

The magnitudes of the cross sections for reaction (4) follow the order, $Li^+ < Na^+ < K^+ \approx Rb^+$. The relative magnitudes of the M^+ cross sections reflect the relative thresholds, which gradually decrease as the ion gets larger. This order of M^+-NMP binding energies is consistent with previous BDE measurements of other metalized amino acids and ligands [1-11,15,61].

3.4. Threshold analysis

UU IR Author Manuscript

The thresholds for reaction (4) for all M^+(NMP) systems were analyzed without and with RRKM lifetime analysis using Eqs. (1) and (2), respectively. Fig. 3 indicates that the model of Eq. (2) reproduces the experimental cross sections over wide ranges of energies, ~ 4 eV for M^+ = Na^+, K^+, and Rb^+, and ~ 9 eV for M^+ = Li^+. Optimized fitting parameters were obtained using the molecular constants of the M^+(NMP) ground states and PSL transition states and are listed in Table 3. The differences between the threshold values obtained without and with the lifetime analyses are the kinetic shifts for the M^+(NMP) systems. Kinetic shifts for M^+ = Na^+, K^+, and Rb^+ were found to be 0.48, 0.29, and 0.16 eV, respectively (slightly lower when the methyl group is treated as a rotor, see below), and cannot be provided for Li^+ because of the complexities of the competitive channels. Kinetic shifts for analogous proline and glycine complexes were 0.20 and 0.04 eV for Na^+, 0.10 and 0.01 eV for K^+, and 0.08 and 0.03 eV for Rb^+. The larger kinetic shifts of M^+(NMP) in comparison to the corresponding M^+(Pro) and M^+(Gly) complexes indicate the importance of incorporating the RRKM theory in the threshold analysis. Kinetic shifts vary among systems depending on the dissociation energy (higher E_0 values lead to larger kinetic shifts) and the complexity of the system (larger ligands yield larger kinetic shifts). Gly is the simplest aliphatic amino acid, and although Pro has the same backbone structure as NMP, the additional methyl group on NMP increases the number of degrees of freedom available for energy randomization to occur.

We also considered whether coordination of the metal to the binding sites in the M^+(NMP) complexes hinders the rotation of the methyl group, an effect that was found to be influential in comparing the dissociation behavior of metallated serine (Ser) and threonine (Thr) [9]. In the ground state zwitterions of M^+(NMP), the metal ion is not in the vicinity of the methyl group, however, the proton on the nitrogen is located such that it prefers to be staggered with respect to the hydrogens of the methyl group. Calculations indicate that the torsional vibration of the methyl group in NMP has a frequency of 228 cm^{-1}. For the ground state conformers of M^+(NMP), this frequency increases to 250 cm^{-1} in Li^+(NMP), 261 cm^{-1} in Na^+(NMP), 258 cm^{-1} in K^+(NMP), and 254 cm^{-1} in Rb^+(NMP), indicating some hindering of the

UU IR Author Manuscript

methyl rotor upon metal cation complexation. Therefore, we also analyzed the data after replacing the torsional vibrational frequency of the methyl group by an internal rotational constant of 5.4 cm^{-1} [62]. This internal rotor treatment was applied to both the M^+(NMP) complex and the NMP product and also to just the NMP product [9]. When the modification was applied to both M^+(NMP) and NMP for $M^+ = Li^+$, Na^+, K^+, and Rb^+, the thresholds shift upward by 0.05, 0.01, 0.01, and 0.00 eV, respectively. When the same modification was applied to NMP alone, the threshold increased systematically by 0.05, 0.07, 0.05, and 0.04 eV, respectively. The latter results show that the internal rotor treatment of the methyl group loosens the PSL TS, thereby reducing the kinetic shift. In all cases, the experimental uncertainties include the values in which the torsion was treated as a vibration.

$\Delta S^{\dagger}_{1000}$, the activation entropy at 1000 K, is also given in Table 3 and characterizes the nature of the transition state. The $\Delta S^{\dagger}_{1000}$ values determined from fitting the data were in the range 40 – 50 J/mol K, within the interval determined by Lifshitz for simple bond cleavage dissociations [63]. This is reasonable considering that the TS is assumed to lie at the centrifugal barrier for the association of M^+ with NMP. When the internal rotor treatment was applied to the methyl group in M^+(NMP) and NMP, the $\Delta S^{\dagger}_{1000}$ values decreased by ~ 1 J/mol K. When the methyl group was treated as an internal rotor in NMP alone, the $\Delta S^{\dagger}_{1000}$ values increased by ~ 7 J/mol K, again indicating a looser TS.

3.5. Conversion to 298 K values

Because most thermodynamic values are tabulated at 298 K, we convert our 0 K bond energies to 298 K bond enthalpies (ΔH) and free energies (ΔG). The values of ΔH_0, ΔH_{298}, and ΔG_{298}, along with the conversion factors are reported in Table 4. The enthalpy conversions and entropy contributions are calculated using standard formulae, and the vibrational frequencies and rotational constants were determined at the B3LYP/6-311+G(d,p) level of theory for Li^+(NMP), Na^+(NMP), and K^+(NMP), and at the B3LYP/def2-TZVP level for Rb^+(NMP). Table 4 shows

UU IR Author Manuscript

thermodynamic values obtained by treating the methyl torsion as a vibration and as an internal rotor in the NMP product for all four metal complexes.

4. Discussion

4.1. Comparison between theoretical and experimental bond dissociation energies

The experimental threshold energies listed in Table 3 are equivalent to the M^+(NMP) bond dissociation energies at 0 K. Table 5 compares theoretical BDEs with the experimental BDEs obtained with and without treating the methyl group as a rotor in the NMP product. Mean absolute deviations (MADs) between the theoretical and experimental BDEs for all four metal complexes are also provided. The value obtained for K^+(NMP) with the methyl group treated as a vibration, 150.6 ± 5.8 kJ/mol, agrees with our preliminary determination of 148.8 ± 7.6 kJ/mol reported previously [22]. The small differences are a result of fitting a more extensive set of data.

All three levels of theory (B3LYP, B3P86, and MP2) give similar BDEs for the M^+(NMP) complexes, as shown in Table 5 and Fig. 4. Values obtained using the def2-TZVPP basis set are generally slightly lower (by an average of 5.3 ± 1.9 kJ/mol) than those for the 6-311+G(2d,2p) basis set and lie an average of 1.7 ± 0.7 kJ/mol below values calculated using the def2-TZVP basis set (not shown in Table 5). The MAD values for the counterpoise corrected MP2(full) bond energies are lower than those for uncorrected values, although the absolute agreement between the MP2(full) BDEs in the case of Li^+(NMP) is better without cp corrections, as previously suggested [54]. The use of core-correlation on Li has little effect (although the MP2 value improves slightly), with geometries calculated at B3LYP and MP2(full) levels giving BDEs within 1 kJ/mol of one another (not shown in Table 5). It seems likely that core-correlation does not greatly affect the present BDEs because NMP is a multi-dentate ligand and the largest effects associated with the core-correlation are found for monodentate ligands as these shorten the lithium-ligand bond distance the most [54]. As also found in previous work with other Na^+(L) complexes [1,2,5,7,9,64], B3LYP tends to overbind, giving a higher value of the sodium binding affinity compared to experiment and the other two theoretical methods. Overall,

UU IR Author Manuscript

the MADs are generally slightly lower for the experimental values obtained when treating the methyl group as a rotor in the products, but the distinction lies within experimental uncertainties. For the cp corrected values at all three levels of theory, the MADs are comparable, in the range 6 – 10 kJ/mol, comparable to the experimental uncertainties. These drop by about 2 kJ/mol when cp corrections are *not* included for Li^+(NMP), as previously recommended [54]. Most importantly, because the lowest energy charge-solvated structures for the M^+(NMP) complexes (either [N, CO] C4-down, t or [COOH] C3-up depending on the metal and level of theory) lie 15 – 37 kJ/mol above the zwitterionic ground states (Table 2), the comparison between our experimental and theoretical BDEs confirms that the M^+(NMP) complexes formed here are zwitterions. This agrees with the IRMPD results for K^+(NMP) [22].

4.2. Comparison between M^+(NMP) and other M^+(AA) complexes – Effect of the methyl group

Compared to M^+(Pro), the binding energies of M^+(NMP) increase by 8, 8, 10, and 5 kJ/mol (~ 3%, 4%, 8%, and 4%) for Li^+, Na^+, K^+, and Rb^+, respectively, when the methyl group in NMP is treated as a rotor. In contrast, when the methyl group torsion is treated as a vibration, the BDEs of the M^+(NMP) complexes increase by 3, 1, 6, and 1 kJ/mol, respectively. We expect that the BDEs of NMP to alkali metal cations should be higher than those to Pro on the basis of the combined effects of the higher polarizability of NMP and the electron-donating effect of the methyl group, as discussed further below. Indeed, theory predicts that the Li^+, Na^+, K^+, and Rb^+ BDEs to NMP should increase by 19 ± 2, 15 ± 1, 15 ± 1, and 10 ± 3 kJ/mol, respectively, compared to M^+(Pro) BDEs calculated at comparable levels. In addition, we can compare these differences with those previously measured for methylation in other systems. For example, Ye et al. and Bowman et al. reported increases of 4 – 6 kJ/mol in the BDEs of M^+(Thr) relative to those of M^+(Ser) [6,9]. Hallowita et al. [65] reported the BDEs of alkali metal cation complexes of *N*,*N*-dimethyl aniline (NNDMA), *N*-methyl aniline (NMA), and compared them to those for aniline (A) from Amunugama and Rodgers [66]. Here, the BDEs of M^+(NNDMA) versus M^+(NMA) and M^+(NMA) versus M^+(A) have an average difference of 6.6 ± 3.0 kJ/mol. Overall,

UU IR Author Manuscript

the increase of 5 – 10 kJ/mol in the M^+(NMP) BDEs upon methylation obtained by treating the methyl group in NMP as a rotor is more consistent with theory and with previous measurements of BDEs of other alkali metal cation methylated ligand complexes. Thus, we believe our best experimental BDEs are the ones obtained by treating the methyl group torsion in the product NMP as a rotor.

Metal ions interact with amino acids via electrostatic ion-dipole, ion induced-dipole, and ion-quadrupole forces that lead to the solvation of the charge by coordination of the functional groups present in the amino acid. As the metal cation is changed from Li^+ to Na^+, the BDE of M^+(NMP) drops by about 93 kJ/mol (~ 32%); from Na^+ to K^+, the BDE decreases by about 39 kJ/mol (~ 20%); and by another 25 kJ/mol (~16%) in moving from K^+ to Rb^+. These changes are comparable to those found previously, about 26 – 33% for Li^+ to Na^+, 23 – 30% for Na^+ to K^+, and 10 – 20% for K^+ to Rb^+, in studies of M^+(Gly), M^+(Pro), M^+(Ser), M^+(Thr), M^+(Met), M^+(Cys), M^+(Asp), M^+(Asn), M^+(Glu), and M^+(Gln) complexes [1,2,4-10]. In all these cases, the declining BDEs going from Li^+ to Rb^+ are a consequence of the decreasing electrostatic interaction of the metal ion with the ligand with increasing bond distance, resulting from the increasing size of the metal ion. Indeed, as noted previously for other amino acids [10,15], the BDEs of M^+(NMP), where $M^+ = Li^+$, Na^+, K^+, and Rb^+ inversely correlate with the metal cationic radii (0.70, 0.98, 1.33, and 1.49 Å [67], respectively). This is shown in Fig. 5 along with data for M^+(Gly) and M^+(Pro) for comparison. The three diagonal lines are regression fits constrained to pass through the origin to the M^+(NMP), M^+(Pro) [2,6], and M^+(Gly) BDEs [1,6,8], with slopes of 156, 190, and 198 Å kJ/mol, respectively. These are an indication of the average increase in the bonding interaction for the three amino acids. Thus NMP binds more strongly to the alkali metal cations than Gly by an average of 26 ± 7% and more strongly than Pro by 6 ± 3%. The latter increase is comparable to those measured for several other methylated species compared to their unmethylated versions: Thr versus Ser, 2 ± 6% [6,9]; NMA versus A, 9 ± 3%; and NNDMA versus NMA, 6 ± 3% [65,66].

Rodgers and Armentrout have shown in the past that there is a linear dependence of the binding of Na^+ and K^+ to amino acids on the polarizability of several amino acids: Gly, Pro, Met, Phe, Tyr, and Trp [10,11,15]. The polarizability of NMP is calculated here to be 12.5 $Å^3$, compared to 11.4 $Å^3$ for Pro [15]. (The isotropic molecular polarizability was calculated at the PBE0/6-311+G(2d,2p) level of theory using the B3LYP/6-311G(d,p) optimized geometries of NMP. Polarizabilities obtained from this level of theory are in good agreement with measured polarizabilities [68].) On the basis of the previously established correlation with polarizability, this increase in the polarizability predicts that the NMP BDEs to Na^+ and K^+ should be ~ 4 and ~ 3 kJ/mol, respectively, stronger than those for Pro, somewhat smaller than the 8 and 10 kJ/mol increases measured here. This enhanced effect of methylation can probably be explained on the basis of the inductive effect of the methyl group, which should enhance the basicity of the tertiary amine, stabilizing the ground state M^+(NMP) zwitterions. This effect can be observed in the calculated M^+─OC bond distances, which decrease in the M^+(NMP) complexes by 0.005 Å relative to those in M^+(Pro) complexes.

5. Conclusions

The kinetic energy dependences of the CID of M^+(NMP), where $M^+ = Li^+$, Na^+, K^+, and Rb^+, were studied using GIBMS. The primary processes observed in Na^+, K^+, and Rb^+ complexes are the loss of the intact ligand. In Li^+(NMP), low-energy decomposition reactions compete with the loss of NMP and are detailed elsewhere [60]. The bond dissociation energies (BDEs) for the loss of NMP from the metallated complexes at 0 K are obtained from a detailed modeling of the experimental cross sections. Experiments show that the binding order of the metal ions to NMP is $Li^+ > Na^+ > K^+ > Rb^+$, which is inversely related to the metal cationic radii. Theoretical BDEs agree well with our experimental bond energies for all four metal systems. This agreement positively identifies these complexes as having structures where the metal cation binds to both carboxylate oxygens of a zwitterionic ligand. Comparison with previous results for M^+(Pro) complexes show that the bond energy of the alkali metal ions to the carboxylate

UU IR Author Manuscript

oxygens is increased slightly by the inductive effect of the methyl group on the ring nitrogen and the increased polarizability. According to theory, one interesting effect of methylation is an *increase* in the number of conformers available to the M^+(NMP) complexes compared to M^+(Pro), whereas one might have imagined that steric constraints would restrict this. In essence, this is because the methyl group can sit on either side of the pyrrolidine ring, with inversion at the nitrogen center being restricted compared to proline.

Acknowledgement

This work has been supported by the National Science Foundation Grant CHE-1049580. The authors would like to thank the Center for High Performance Computing (CHPC) at the University of Utah for generous computational time. The authors also thank Mathias Schäfer and Miriam Drayss for providing us with the sample of NMP and the calculations on K^+(NMP). Finally, AM thanks Amy A. Clark for help with acquiring the data on the GIBMS.

Appendix A. Supplementary data

Supplementary data associated with this article can be found, in the online version, at http://dx.doi.org/xxx.

References

[1] R.M. Moision, P.B. Armentrout, J. Phys. Chem. A 106 (2002) 10350.
[2] R.M. Moision, P.B. Armentrout, J. Am. Chem. Soc. 110 (2006) 3933.
[3] S.J. Ye, P.B. Armentrout, J. Phys. Chem. B 112 (2008) 10303.
[4] A.L. Heaton, P.B. Armentrout, J. Phys. Chem. B 112 (2008) 12056.
[5] A.L. Heaton, R.M. Moision, P.B. Armentrout, J. Phys. Chem. B 112 (2008) 3319.
[6] V.N. Bowman, A.L. Heaton, P.B. Armentrout, J. Phys. Chem. B 114 (2010) 4107.
[7] P.B. Armentrout, E.I. Armentrout, A.A. Clark, T.E. Cooper, E.M.S. Stennett, D.R. Carl, J. Phys. Chem. B 114 (2010) 3927.
[8] R.M. Moision, P.B. Armentrout, Phys. Chem. Chem. Phys. 6 (2004) 2588.
[9] S.J. Ye, A.A. Clark, P.B. Armentrout, J. Phys. Chem. B 112 (2008) 10291.
[10] P.B. Armentrout, A. Gabriel, R.M. Moision, Int. J. Mass Spectrom. 283 (2009) 56.
[11] C. Ruan, M.T. Rodgers, J. Am. Chem. Soc. 126 (2004) 14600.
[12] M.T. Rodgers, P.B. Armentrout, Mass Spectrom. Rev. 19 (2000) 215.

UU IR Author Manuscript

[13] P.B. Armentrout, Int. J. Mass Spectrom. 200 (2000) 219.
[14] P.B. Armentrout, J. Am. Soc. Mass Spectrom. 13 (2002) 419.
[15] M.T. Rodgers, P.B. Armentrout, Acc. Chem. Res. 37 (2004) 989.
[16] G. Blunden, A.V. Patel, M. Adrian-Romero, P. Meléndez, Biochem. Syst. Ecol. 32 (2004) 1153.
[17] R.R. Pfister, J.L. Haddox, C.I. Sommers, K.-W. La, Invest. Ophthalmol. Vis. Sci. 36 (1995) 1306.
[18] C. Kapota, J. Lemaire, P. Maitre, G. Ohanessian, J. Am. Chem. Soc. 126 (2004) 1836.
[19] M.K. Drayß, D. Blunk, J. Oomens, M. Schäfer, J. Phys. Chem. A 112 (2008) 11972.
[20] M.K. Drayß, D. Blunk, J. Oomens, B. Gao, T. Wyttenbach, M.T. Bowers, M. Schäfer, J. Phys. Chem. A 113 (2009) 9543.
[21] M.K. Drayß, P.B. Armentrout, J. Oomens, M. Schäfer, Int. J. Mass Spectrom. 297 (2010) 18.
[22] M. Schäfer, M.K. Drayss, D. Blunk, J.M. Purcell, C.L. Hendrickson, A.G. Marshall, A. Mookherjee, P.B. Armentrout, J. Phys. Chem. A 113 (2009) 7779.
[23] K.M. Ervin, P.B. Armentrout, J. Chem. Phys. 83 (1985) 166.
[24] F. Muntean, P.B. Armentrout, J. Chem. Phys. 115 (2001) 1213.
[25] R.M. Moision, P.B. Armentrout, J. Am. Soc. Mass. Spectrom. 18 (2007) 1124.
[26] T. Kim, A.V. Tolmachev, R. Harkewicz, D.C. Prior, G. Anderson, H.R. Udseth, R.D. Smith, Anal. Chem. 72 (2000) 2247.
[27] S.J. Ye, P.B. Armentrout, J. Phys. Chem. A 112 (2008) 3587.
[28] D.R. Carl, R.M. Moision, P.B. Armentrout, Int. J. Mass Spectrom. 265 (2007) 308.
[29] E. Teloy, D. Gerlich, Chem. Phys. 4 (1974) 417.
[30] D. Gerlich, Adv. Chem. Phys. 82 (1992) 1.
[31] N. Aristov, P.B. Armentrout, J. Phys. Chem. 90 (1986) 5135.
[32] N.F. Dalleska, K. Honma, L.S. Sunderlin, P.B. Armentrout, J. Am. Chem. Soc. 116 (1994) 3519.
[33] N.R. Daly, Rev. Sci. Instrum. 31 (1960) 264.
[34] T.S. Beyer, D.F. Swinehart, Comm. Assoc. Comput. Machines 16 (1973) 379.
[35] S.E. Stein, B.S. Rabinovich, Chem. Phys. Lett. 49 (1977) 1883.
[36] M.T. Rodgers, K.M. Ervin, P.B. Armentrout, J. Chem. Phys. 106 (1997) 4499.
[37] K.A. Holbrook, M.J. Pilling, S.H. Robertson, Unimolecular Reactions, John Wiley & Sons Ltd., New York, 1996.
[38] R.G. Gilbert, S.C. Smith, Theory of Unimolecular and Recombination reactions, Blackwell Scientific, Oxford, 1990.
[39] P.B. Armentrout, J. Simons, J. Am. Chem. Soc. 114 (1992) 8627.
[40] M.T. Rodgers, P.B. Armentrout, J. Chem. Phys. 109 (1998) 1787.
[41] P.B. Armentrout, K.M. Ervin, M.T. Rodgers, J. Phys. Chem. A 112 (2008) 10071.
[42] D.A. Hales, L. Lian, P.B. Armentrout, Int. J. Mass Spectrom. Ion Proc. 102 (1990) 269.
[43] P.J. Chantry, J. Chem. Phys. 55 (1971) 2746.
[44] C. Lifshitz, R.L.C. Wu, T.O. Tiernan, D.T. Terwilliger, J. Chem. Phys. 68 (1978) 247.
[45] M.J. Frisch, G.W. Trucks, H.B. Schlegel, G.E. Scuseria, M.A. Robb, J.R. Cheeseman, G. Scalmani, V. Barone, B. Mennucci, G.A. Petersson, H. Nakatsuji, M. Caricato, X. Li, H.P. Hratchian, A.F. Izmaylov, J. Bloino, G. Zheng, J.L. Sonnenberg, M. Hada, M. Ehara, K. Toyota, R. Fukuda, J. Hasegawa, M. Ishida, T. Nakajima, Y. Honda, O. Kitao, H. Nakai, T. Vreven, J.A. Montgomery, J. Peralta, J. E.; , F. Ogliaro, M. Bearpark, J.J.

Heyd, E. Brothers, K.N. Kudin, V.N. Staroverov, R. Kobayashi, J. Normand, K. Raghavachari, A. Rendell, J.C. Burant, S.S. Iyengar, J. Tomasi, M. Cossi, N. Rega, J.M. Millam, M. Klene, J.E. Knox, J.B. Cross, V. Bakken, C. Adamo, J. Jaramillo, R. Gomperts, R.E. Stratmann, O. Yazyev, A.J. Austin, R. Cammi, C. Pomelli, J.W. Ochterski, R.L. Martin, K. Morokuma, V.G. Zakrzewski, G.A. Voth, P. Salvador, J.J. Dannenberg, S. Dapprich, A.D. Daniels, Ö. Farkas, J.B. Foresman, J.V. Ortiz, J. Cioslowski, D.J. Fox, Gaussian 09, Revision A.01. Gaussian, Inc.: Pittsburg, PA, 2009.

[46] F. Weigend, R. Ahlrichs, Phys. Chem. Chem. Phys. 7 (2005) 3297.

[47] T. Leininger, A. Nicklass, W. Küchle, H. Stoll, M. Dolg, A. Bergner, Chem. Phys. Lett. 255 (1996) 274.

[48] J.B. Foresman, A.E. Frisch, Exploring Chemistry with Electronic Structure Methods, Gaussian Inc., Pittsburg PA, 1996.

[49] D. Feller, J. Comp. Chem. 17 (1996) 1571.

[50] K.L. Schuchardt, B.T. Didier, T. Elsethagen, L. Sun, V. Gurumoorthi, J. Chase, Li, J. , T.L. Windus, J. Chem. Inf. Model. 47 (2007) 1045.

[51] F.B. van Duijneveldt, J.G.C.M. van Duijneveldt-van de Rijdt, J.H. van Lenthe, Chem. Rev. 94 (1994) 1873.

[52] D. Feller, E.D. Glendening, D.E. Woon, J. Chem. Phys. 103 (1995) 3526.

[53] D. Feller, Chem. Phys. Lett. 322 (2000) 543.

[54] M.T. Rodgers, P.B. Armentrout, Int. J. Mass Spectrom. 267 (2007) 167.

[55] T.H.J. Dunning, J. Chem. Phys. 90 (1989) 1007.

[56] R.A. Kendall, T.H.J. Dunning, R.J. Harrison, J. Chem. Phys. 96 (1992) 6976.

[57] J. Bertran, L. Rodrıguez-Santiago, M. Sodupe, J. Phys. Chem. B 103 (1999) 2310.

[58] L. Rodriguez-Santiago, M. Sodupe, J. Tortajada, J. Phys. Chem. A 105 (2001) 5340.

[59] P.B. Armentrout, A.L. Heaton, S.J. Ye, J. Phys. Chem. A 115 (2011) 11144.

[60] A. Mookherjee, P.B. Armentrout, work in progress.

[61] Z. Yang, M.T. Rodgers, Phys. Chem. Chem. Phys. 14 (2012) 4517.

[62] L.H. Sprangler, Annu. Rev. Phys. Chem. 48 (1997) 481.

[63] C. Lifshitz, Adv. Mass Spectrom. 11 (1989) 713.

[64] P.B. Armentrout, M.T. Rodgers, J. Phys. Chem. A 104 (1999) 2238.

[65] N. Hallowita, D.R. Carl, P.B. Armentrout, M.T. Rodgers, J. Phys. Chem. A 112 (2008) 7996.

[66] R. Amunugama, M.T. Rodgers, Int. J. Mass Spectrom. 227 (2003) 339.

[67] R.G. Wilson, G.R. Brewer, Ion Beams with Applications to Ion Implantation, Wiley, New York, 1973.

[68] S.M. Smith, A.N. Markevitch, D.A. Romanov, X. Li, R.J. Levis, H.B. Schlegel, J. Phys. Chem. A 108 (2004) 11063.

Table 1

B3LYP, B3P86 and MP2(full) Relative Energies (kJ/mol) at 0 K of NMP conformers

bonding model[a]	ring structure[b]	Relative Energies[c]		
		B3LYP	B3P86	MP2(full)
N2	C3-up	0.0 (0.0)	0.0 (0.0)	0.0 (0.0)
N2	C2-up	5.9 (5.5)	6.5 (6.2)	6.5 (5.9)
N1	N-up	9.9 (8.9)	12.7 (12.6)	11.6 (11.8)
N3	C3-up	11.2 (9.5)	13.9 (13.3)	12.4 (12.9)
N1	C1-up	11.5 (10.8)	14.1 (14.1)	11.1 (12.4)
N3	N-up	11.8 (11.1)	14.5 (14.8)	13.3 (13.8)
N1	C3-up	13.1 (11.8)	16.9 (15.8)	13.9 (14.9)
N3	C1-up	14.8 (13.9)	17.4 (17.5)	13.6 (15.7)
N2	N-up	36.8 (36.7)	36.3 (36.8)	30.2 (30.5)

[a]See text.

[b]Position of pucker in the ring.

[c]All structures are geometry optimized and have zero point energy corrections calculated at the B3LYP/6-311+G(d,p) level. Single point energies at the three levels indicated were calculated using the 6-311+G(2d,2p) basis set. Values within parenthesis were calculated using the def2-TZVP basis set for both B3LYP geometry optimizations and single point energies at the level indicated.

Table 2

B3LYP, B3P86, and MP2(full) 0 K Relative Energies (kJ/mol) of M^+(NMP) conformers

structure		Li^+(NMP)[a]	Na^+(NMP)[b]	K^+(NMP)[b]	Rb^+(NMP)[b]
[CO_2^-]	C3-up	0.0, 0.0, 0.0	0.0, 0.0, 0.0,	0.0, 0.0, 0.0,	
			(0.0, 0.0, 0.0)	(0.0, 0.0, 0.0)	(0.0, 0.0, 0.0)
	C3-down	2.7, 3.9, 5.2	4.1, 4.9, 5.4	4.3, 5.3, 5.9	
			(4.2, 4.9, 5.4)	(4.8, 5.5, 6.1)	(4.9, 5.7, 6.3)
	N-up	32.1, 33.5, 30.8	34.6, 35.8, 32.3	36.9, 38.5, 34.9	
			(35.2, 36.5, 33.0)	(38.2, 39.7, 36.3)	(39.3, 40.8, 37.5)
	C1-up	33.4, 35.1, 29.9	40.1, 41.7, 36.9	37.6, 39.6, 35.3	
			(35.3, 37.2, 33.1)	(38.6, 40.6, 36.6)	(39.8, 41.9, 38.0)
[COOH]	C3-up	[CO_2^-] C3-up	36.7, 31.4, 35.9	26.8, 23.1, 26.2	
			([CO_2^-] C3-up)	(22.4, 19.3, 22.5)	(17.5, 15.1, 18.6)
	C3-down	[CO_2^-] C3-down	43.4, 38.4, 43.6	32.4, 30.0, 33.7	
			([CO_2^-] C3-down)	(29.1, 26.5, 29.8)	(24.2, 22.4, 26.1)
	N-up	113.8, 109.1, 109.3	93.7, 90.2, 88.2	77.6, 76.3, 73.3	
			(92.4, 88.8, 87.2)	(75.3, 73.7, 71.8)	(69.1, 68.1, 66.9)
[N, CO]	C4-down, t	23.7, 25.1, 32.2	37.3, 37.6, 38.5	36.9, 38.1, 36.7	
			(34.9, 35.1, 35.4)	(34.9, 35.9, 34.1)	(33.9, 35.3, 32.6)
	C4-down, c	43.9, 44.7, 52.7	57.9, 57.0, 59.2	56.9, 56.8, 56.2	
			(55.5, 5.2, 57.0)	(53.8, 54.5, 54.8)	(52.3, 53.6, 53.3)
	N-up, t	60.4, 58.4, 59.2	65.7, 63.9, 60.8	63.7, 62.6, 57.1	
			(64.8, 62.7, 58.1)	(62.0, 60.9, 54.8)	(60.2, 59.4, 52.2)
	N-up, c	70.4, 77.0, 78.0	86.4, 83.0, 80.8	83.4, 80.8, 76.4	
			(84.9, 81.9, 79.2)	(86.4, 83.0, 80.8)	(78.7, 77.2, 72.3)

[N, OH]	N-up	65.4, 65.0, 67.5[c]	76.3, 77.1, 70.4	74.1, 75.2, 66.2	
			(74.1, 75.7, 68.4)	(71.2, 73.4, 64.5)	(69.2, 71.5, 62.3)
[CO]	C1-up, t	[N, CO] C4-down, t	85.4, 86.7, 94.5	72.6, 75.6, 79.4	
				(67.9, 70.7, 78.4)	(62.2, 65.5, 72.3)
	C1-up, c	105.0, 105.3, 116.3	93.8, 92.7, 99.8	75.8, 78.4, 83.6	
			(89.1, 88.9, 100.5)	(72.2, 74.3, 83.6)	(65.8, 68.6, 77.2)

[a]B3LYP, B3P86, and MP2(full) single point energies calculated using the aug-cc-pVTZ(Li-C) basis set with geometries and zero-point corrections calculated at the MP2(full)/cc-pVDZ(Li-C) level.

[b]B3LYP, B3P86 and MP2(full) single point energies calculated using the 6-311+G(2d,2p) basis sets with structures and zero-point energies at the B3LYP/6-311+G(d,p) level of theory. Values in parentheses show B3LYP, B3P86 and MP2(full) single point energies calculated using the def2-TZVP basis set, with geometries and zero-point corrections calculated at the B3LYP/def2-TZVP level of theory.

[c] The dihedrals for this molecule change the designation to C4-down.

UU IR Author Manuscript

Table 3

Fitting parameters of Eqs. (1) and (2), Threshold Dissociation Energies at 0 K, and Entropies of Activation at 1000 K for CID of M^+(NMP) with Xe[a]

reactant	prod.		n	E_0 [b] (eV)	E_0 (PSL)[c] (eV)	E_0 (PSL)[d] (eV)	$\Delta S^{\ddagger}_{1000}$[c] (J/molK)	$\Delta S^{\ddagger}_{1000}$[d] (J/molK)
Li^+(NMP)	Li^+	12. 6	0.9		2.92	2.97	42 (2)	49 (4)
		(1.8)	(0.1)		(0.08)	(0.08)		
Na^+(NMP)	Na^+	3.2	1.9	2.42	1.94	2.01	41 (2)	48 (4)
		(0.7)	(0.2)	(0.1)	(0.09)	(0.09)		
K^+(NMP)	K^+	11.1	1.2	1.84	1.56	1.60	35 (3)	42 (4)
		(0.9)	(0.1)	(0.08)	(0.06)	(0.06)		
Rb^+(NMP)	Rb^+	5.3	1.6	1.47	1.31	1.35	33 (3)	39 (4)
		(0.8)	(0.1)	(0.09)	(0.06)	(0.06)		

[a]Uncertainties are listed in parentheses.

[b]Lifetime effects not included.

[c]Methyl group in NMP treated as a vibration.

[d]Methyl group in NMP treated as an internal rotor.

UU IR Author Manuscript

Table 4

Enthalpies and Free Energies of M^+(NMP) Binding at 0 and 298 K in kJ/mol[a]

complex	ΔH_0[b]	$\Delta H_{298} - \Delta H_0$[c]	ΔH_{298}	$T\Delta S_{298}$[c]	ΔG_{298}
Li^+(NMP)	281.9 (7.3)	3.3 (1.6)	285.1 (7.5)	33.3 (4.6)	251.8 (8.8)
	286.7 (7.3)	*3.1 (1.7)*	*289.9 (7.5)*	*38.1 (4.6)*	*251.7 (8.8)*
Na^+(NMP)	187.2 (9.0)	1.9 (1.2)	189.1 (9.1)	32.6 (4.9)	156.4 (10.3)
	194.4 (9.2)	*1.7 (1.3)*	*196.1 (9.3)*	*37.3 (4.9)*	*158.7 (10.5)*
K^+(NMP)	150.6 (5.8)	1.2 (1.0)	151.8 (5.9)	30.8 (4.8)	120.9(7.7)
	154.8 (5.5)	*1.1 (1.0)*	*155.9 (5.6)*	*35.6 (4.9)*	*120.2 (7.4)*
Rb^+(NMP)	126.1 (5.9)	0.9 (0.9)	126.9 (5.9)	30.3 (5.1)	96.6 (7.9)
	130.0 (5.9)	*0.7 (0.9)*	*130.8 (6.0)*	*35.0 (5.1)*	*95.6 (7.9)*

[a]Uncertainities are listed in parenthesis.

[b]Experimental values from Table 1, where the methyl torsion in the NMP product was treated as a vibration (roman) and rotor (italics).

[c]Values computed from standard formulae and molecular constants calculated at the B3LYP/6-311+G(d,p) and B3LYP/def2-TZVP (Rb^+) levels. Uncertainties correspond to 10% variation in vibrational frequencies and a two-fold variation in the metal-ligand frequencies.

UU IR Author Manuscript

Table 5

Experimental and Theoretical Bond Dissociation Energies at 0 K of M^+(NMP)

M^+	expt.[a]	Theory			
		B3LYP(cp)	B3P86(cp)	MP2(full, cp)	MP2(full)
Li^+	281.9 (7.3)	281.1,[b] 281.6,[c]	272.1,[b] 272.4,[c]	268.7,[b] 273.8,[c]	277.9,[b] 277.3,[c]
	286.7 (7.3)	277.3[d]	267.4[d]	264.1[d]	269.7[d]
Na^+	187.2 (9.0)	210.1[b]	202.7[b]	200.1[b]	209.2[b]
	194.4 (9.2)	205.2[d]	197.6[d]	197.5[d]	205.9[d]
K^+	150.6 (5.8)	155.1[b]	155.5[b]	153.7[b]	160.2[b]
	154.8 (5.5)	148.2[d]	146.5[d]	147.8[d]	155.9[d]
Rb^+	126.1 (5.9)	131.1[d]	130.6[d]	134.4[d]	143.9[d]
	129.9 (5.9)				
MAD[e]		8 (10), *6 (7)*[b]	9 (5), *6 (7)*[b]	9 (5), *7 (7)*[b]	13 (8), *11 (4)*[b]
				7 (5), *5 (3)*[b,f]	
		8 (7), *7 (4)*[d]	8 (5), *8 (8)*[d]	10 (6), *9 (9)*[d]	14 (6), *11 (7)*[d]
				8 (4), *8 (6)*[d,f]	

[a] Values from Table 3. Uncertainties are listed in parentheses. Values are obtained by treating the methyl group of the NMP product as a vibration (roman) or as a rotor (italics).

[b] Geometry optimizations and zero-point corrections done at the B3LYP/6-11+G(d,p) level, with final energies taken from single point energies calculated at the corresponding levels using the 6-311+G(2d,2p) basis sets. Counterpoise corrections included (cp).

[c] Values calculated at the indicated levels using the aug-cc-pVTZ(Li-C) basis set, using geometry optimizations and zero-point corrections calculated at the B3LYP/cc-pVDZ(Li-C) level.

[d] Values calculated at the indicated levels using def2-TZVPP basis set, with geometries and zero-point corrections calculated at the B3LYP/def2-TZVPP level.

[e] Mean absolute deviations from experimental BDEs. Values marked with the *b* footnote include the def2-TZVPP values for Rb^+.

[f] Values calculated with no counterpoise correction for Li^+.

Figure Captions

Fig. 1. NMP conformers calculated at the B3LYP/6-311+G(d,p) level. Relative 0 K energies (kJ/mol) calculated at B3LYP, B3P86, and MP2(full) levels using the 6-311+G(2d,2p) basis set are in parenthesis. Dashed lines indicate hydrogen bond lengths in Å.

Fig. 2. Na^+(NMP) conformers calculated at the B3LYP/6-311+G(d,p) level. Dashed lines indicate hydrogen bond lengths in Å for M^+(NMP) in the order: $M^+ = Li^+$, Na^+, K^+, and Rb^+. When only three bond lengths are shown, the value for Li^+ is absent.

Fig. 3. Zero pressure extrapolated cross sections (open circles) for CID of M^+(NMP) with Xe as a function of kinetic energy in the center-of-mass frame (lower x-axis) and the laboratory frame (upper x-axis) for (a) Li^+(NMP), (b) Na^+(NMP), (c) K^+(NMP), and (d) Rb^+(NMP) where NMP = N-methyl proline. Solid lines show the best fit to the experimental data using the model of Eq. (2) convoluted over the neutral and ion kinetic and internal energy distributions. Dashed lines show the model cross sections in the absence of experimental kinetic energy broadening for reactants with an internal energy of 0 K.

Fig. 4. Experimental (methyl rotor treatment) versus theoretical 0 K bond dissociation energies (kJ/mol) of the M^+(NMP) complexes taken from Table 5. Theoretical values using the 6-311+G(2d,2p) basis set (def2-TZVPP for Rb^+) include MP2 (full) (open inverted triangle) without cp corrections, MP2 (full) with cp corrections (open triangle), B3LYP with cp corrections (open circle), and B3P86 with cp corrections (open square) levels. Horizontal error bars are the uncertainties for the experimental BDE values. The diagonal line indicates the values for which measured and calculated BDEs are equal.

Fig. 5. Bond dissociation energies of M^+(AA), where AA = Gly [1,6,8], Pro [2,6], and NMP versus the inverse of the ionic radii of group 1 metals: $M^+ = Li^+$, Na^+, K^+, and Rb^+. The lines are linear regression fits to the M^+(Gly), M^+(Pro), and M^+(NMP) data constrained to pass through the origin.

UU IR Author Manuscript

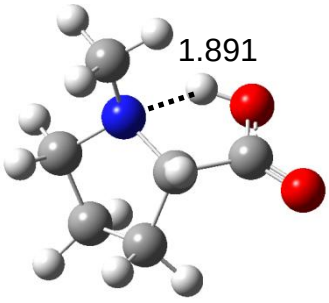

(0.0, 0.0, 0.0)
N2 C3-up

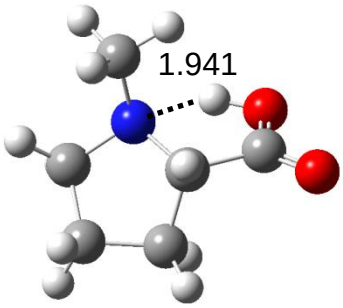

(5.9, 6.5, 6.5)
N2 C2-up

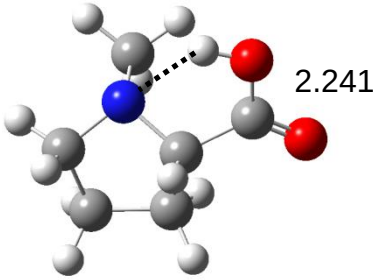

(36.8, 36.3, 30.2)
N2 N-up

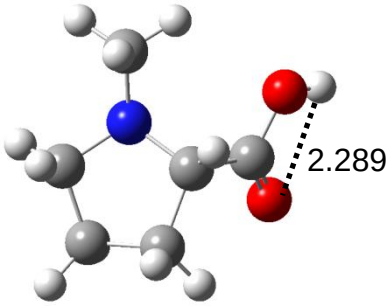

(11.2, 13.9, 12.4)
N3 C3-up

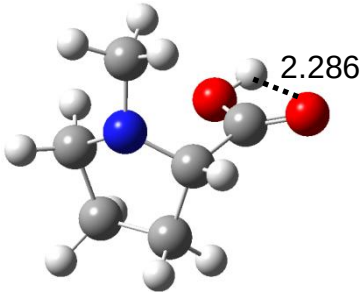

(14.8, 17.4, 13.6)
N3 C1-up

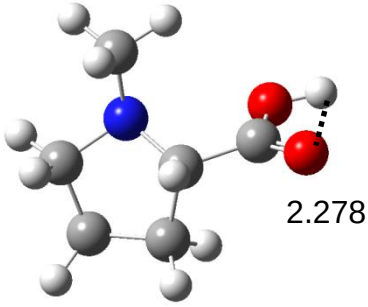

(11.8, 14.5, 13.3)
N3 N-up

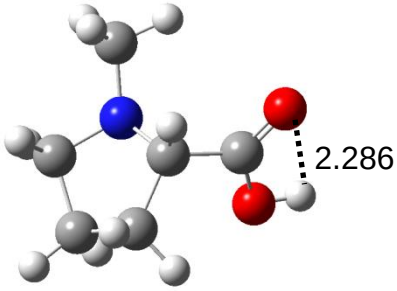

(13.1, 16.9, 13.9)
N1 C3-up

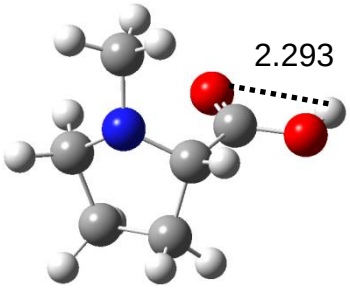

(11.5, 14.1, 11.1)
N1 C1-up

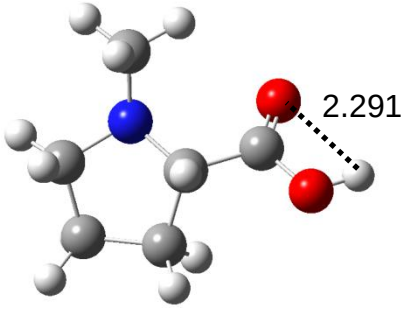

(9.9, 12.7, 11.6)
N1 N-up

Figure 1

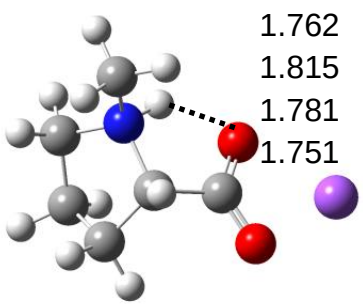

[CO_2^-] C3-up

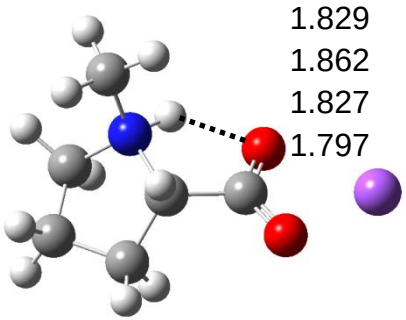

[CO_2^-] C3-down

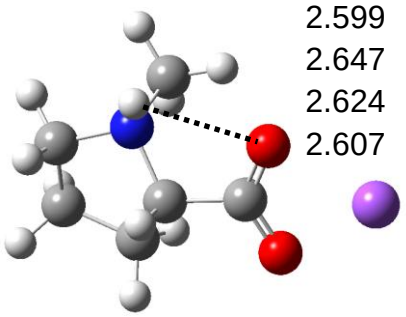

[CO_2^-] N-up

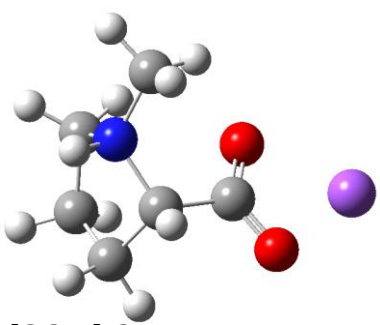

[CO_2^-] C1-up

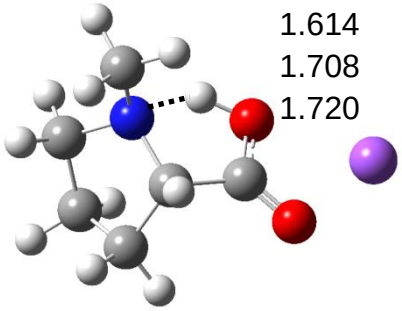

[COOH] C3-up

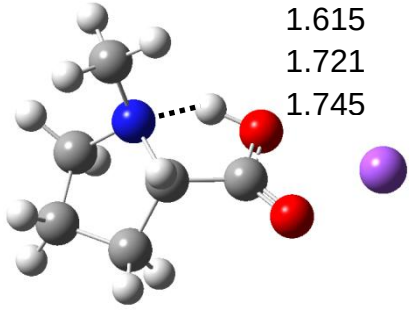

[COOH] C3-down

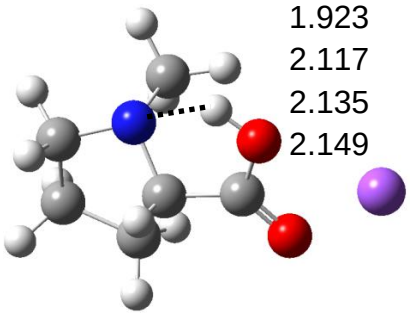

[COOH] N-up

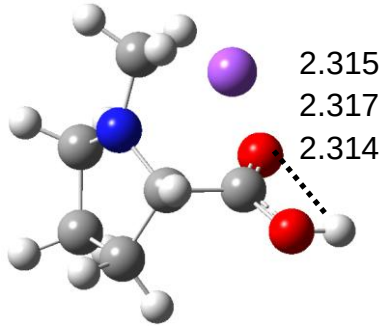

[CO] C1-up, t

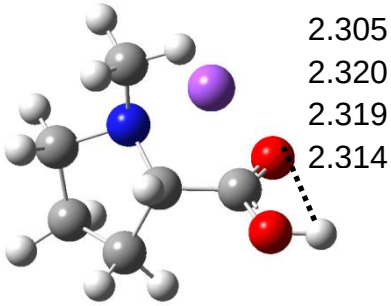

[N, CO] C4-down, t

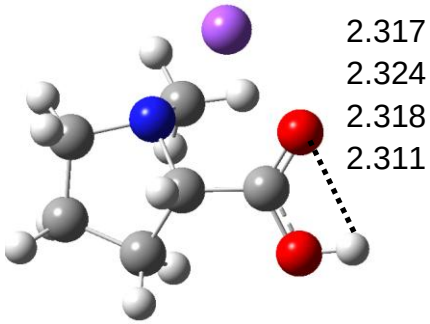

[N, CO] N-up, t

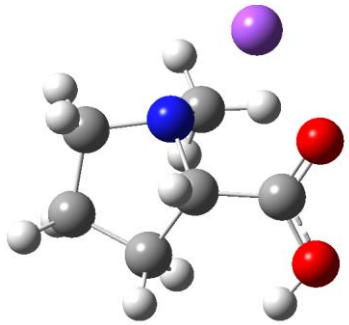

[N, CO] N-up, c

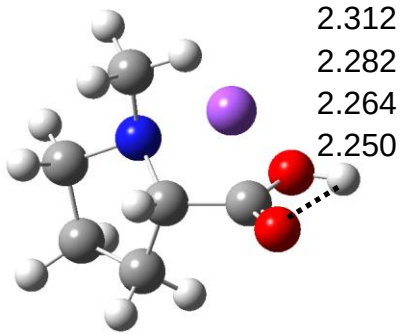

[N, OH] N-up (Li^+ C4-down)

Figure 2

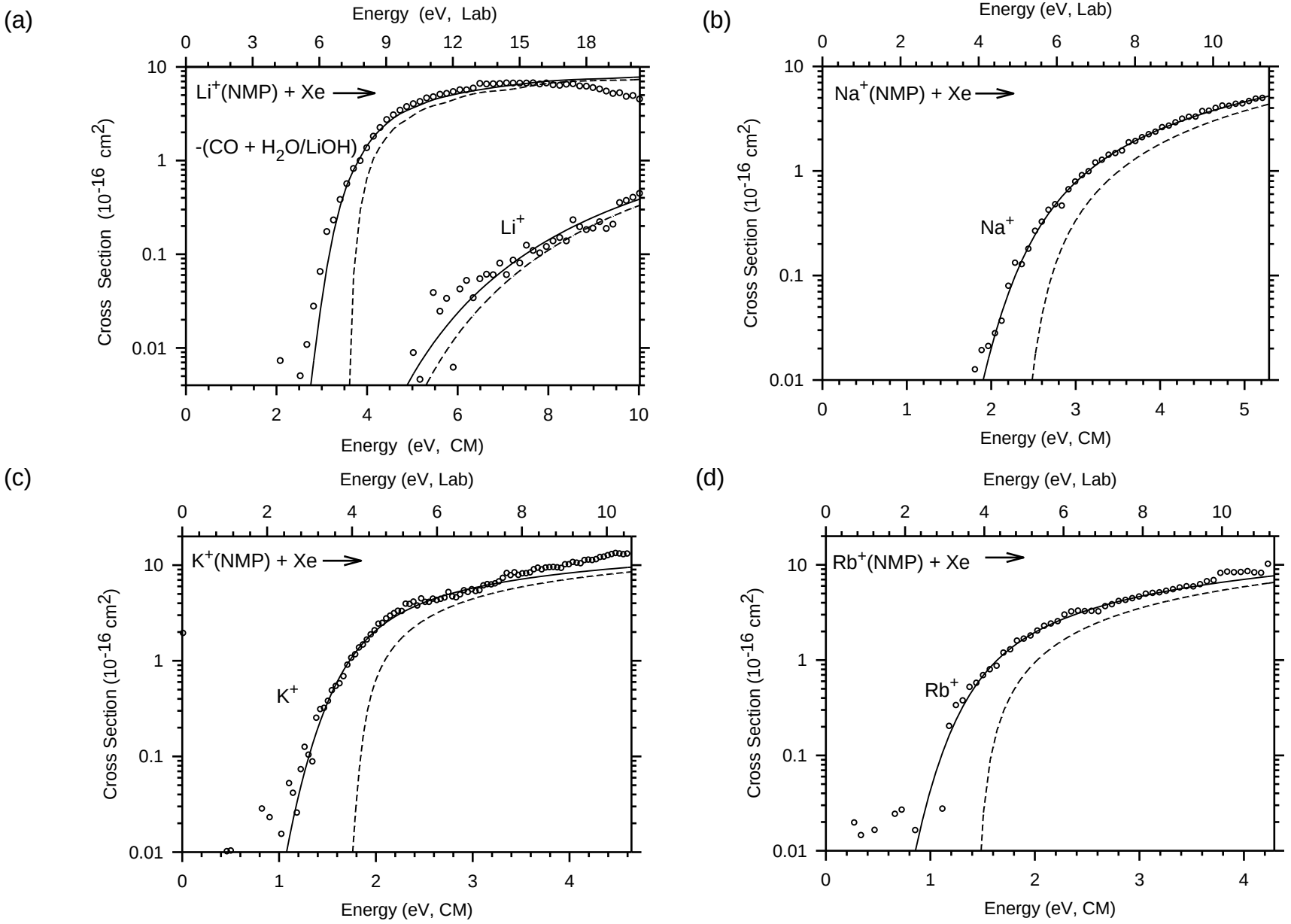
(a)
Energy (eV, Lab)
Li+(NMP) + Xe
-(CO + H2O/LiOH)
Li+
Cross Section (10-16 cm2)
Energy (eV, CM)
(b)
Energy (eV, Lab)
Na+(NMP) + Xe
Na+
Cross Section (10-16 cm2)
Energy (eV, CM)
(c)
Energy (eV, Lab)
K+(NMP) + Xe
K+
Cross Section (10-16 cm2)
Energy (eV, CM)
(d)
Energy (eV, Lab)
Rb+(NMP) + Xe
Rb+
Cross Section (10-16 cm2)
Energy (eV, CM)

Figure 3

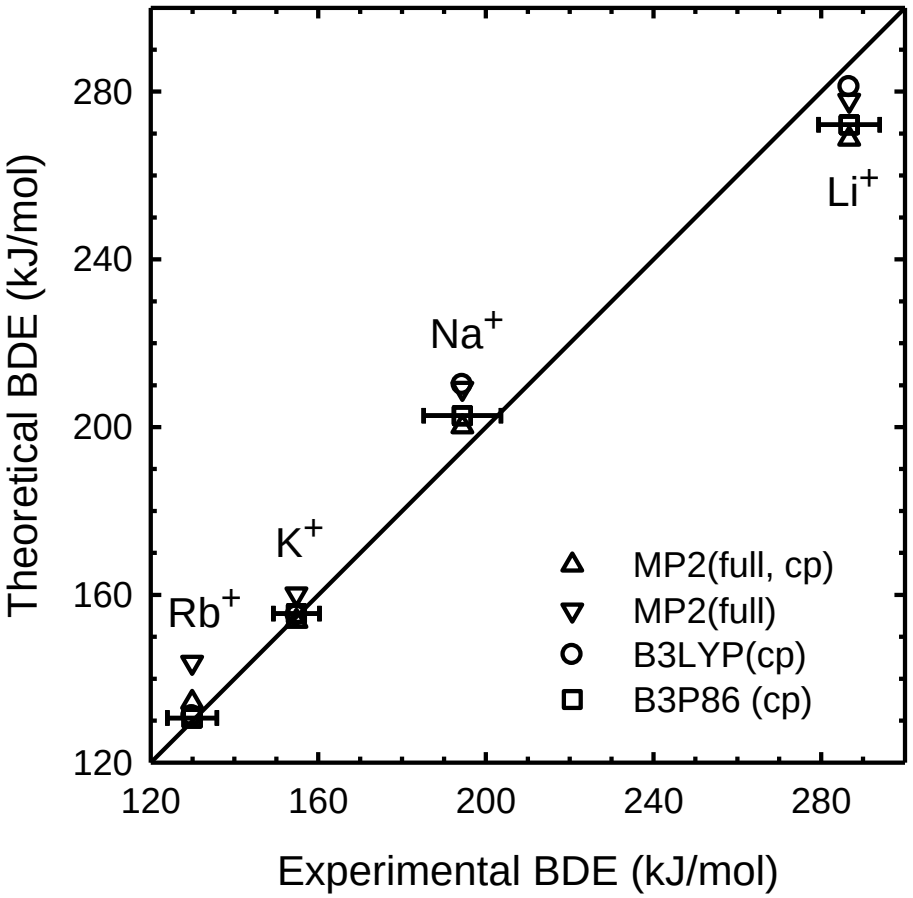

Figure 4

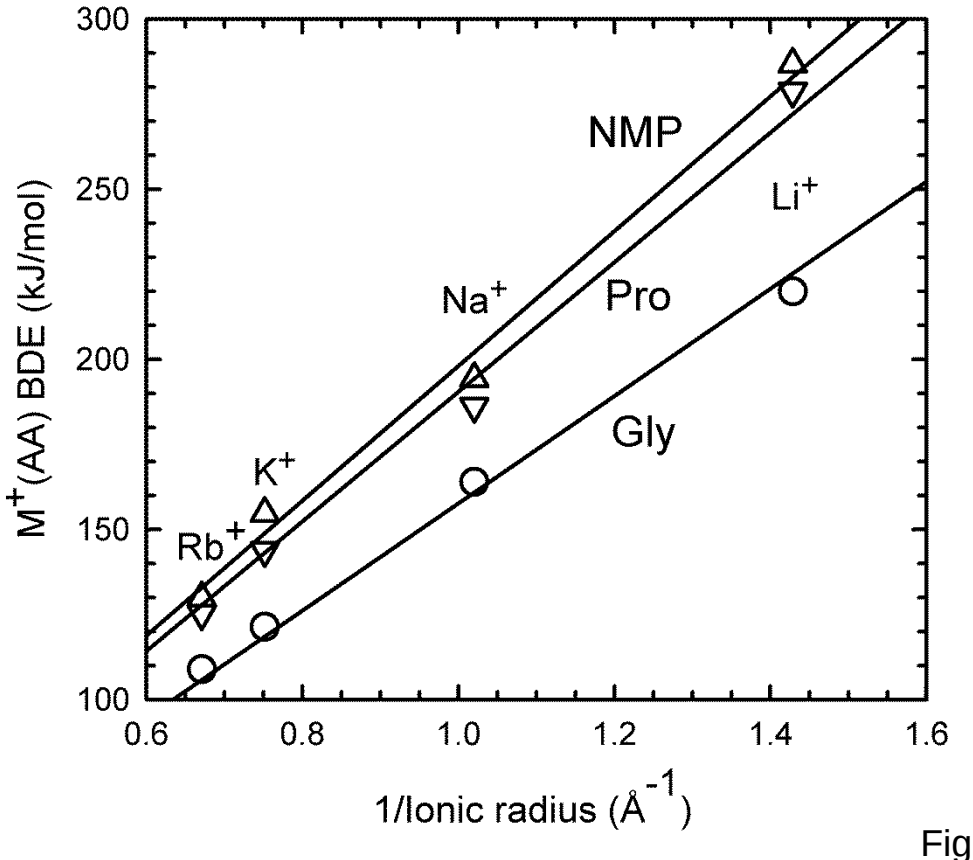

Figure 5

UU IR Author Manuscript

Supplementary Data

Role of Methylation on the Thermochemistry of Alkali Metal Cation Complexes of Amino Acids: N-Methyl Proline

by A. Mookherjee and P. B. Armentrout

Table S1: Vibrational Frequencies Calculated at the B3LYP/6-311+G(d,p) Level

species	Frequencies (cm^{-1})
NMP	52, 98, 193, 203, 228, 293, 319, 399, 480, 574, 597, 617, 739, 819, 872, 885, 894, 924, 940, 970, 1041, 1052, 1106, 1134, 1151, 1173, 1216, 1227, 1237, 1270, 1304, 1324, 1336, 1349, 1382, 1382, 1419, 1463, 1495, 1497, 1503, 1509, 1528, 1834, 2945, 2957, 3032, 3046, 3057, 3066, 3068, 3100, 3104, 3116, 3396
Li^+(NMP)	57, 85, 146, 182, 207, 262, 285, 325, 335, 459, 484, 532, 563, 606, 677, 784, 870, 876, 898, 943, 952, 985, 1031, 1067, 1084, 1112, 1129, 1192, 1213, 1234, 1274, 1291, 1311, 1326, 1364, 1377, 1408, 1454, 1459, 1479, 1487, 1492, 1499, 1510, 1524, 1715, 3111, 3120, 3122, 3126, 3132, 3168, 3200, 3206, 3213, 3242, 3245
Na^+(NMP)	51, 76, 112, 126, 189, 235, 249, 261, 299, 348, 462, 486, 568, 604, 659, 777, 841, 857, 875, 923, 934, 959, 1005, 1038, 1073, 1087, 1128, 1181, 1201, 1229, 1273, 1292, 1316, 1332, 1361, 1378, 1403, 1407, 1463, 1487, 1497, 1499, 1503, 1517, 1524, 1677, 3057, 3064, 3065, 3076, 3111, 3119, 3122, 3132, 3139, 3154, 3159
K^+(NMP)	46, 64, 92, 109, 168, 201, 233, 258, 296, 332, 461, 484, 567, 603, 652, 774, 842, 851, 876, 922, 929, 956, 1006, 1039, 1075, 1088, 1128, 1181, 1201, 1229, 1272, 1290, 1314, 1331, 1359, 1375, 1391, 1405, 1464, 1490, 1497, 1500, 1502, 1516, 1529, 1688, 3052, 3056, 3063, 3067, 3077, 3114, 3118, 3130, 3136, 3152, 3157
Rb^+(NMP)	41, 59, 76, 107, 132, 191, 228, 254, 294, 329, 461, 485, 568, 605, 652, 775, 844, 850, 879, 924, 928, 956, 1009, 1042, 1079, 1091, 1129, 1183, 1202, 1231, 1272, 1289, 1315, 1334, 1359, 1374, 1385, 1404, 1467, 1493, 1499, 1501, 1504, 1517, 1534, 1696, 2990, 3060, 3067, 3069, 3078, 3118, 3122, 3133, 3137, 3152, 3158

Table S2: Rotational Constants (cm^{-1}) Calculated at the B3LYP/6-311+G(d,p) Level of Theory

species	1-D	2-D
NMP	0.0781	0.0419
Li^+(NMP)	0.0745	0.0349
Na^+(NMP)	0.0715	0.0239
K^+(NMP)	0.0700	0.0175
Rb^+(NMP)	0.0695	0.0115

Table S3. Bond distances, and dihedral angles of M^+(NMP) conformers.[a]

Species	r(M^+— O) (Å)	r(M^+— X) (Å)	hydrogen bond (Å)	∠HOCC (deg)	∠CCNC (deg)
[CO_2^-]	1.967	1.994	1.762	-0.1	-114.1
C3-up[b]	2.271 (2.249)	2.319 (2.307)	1.816 (1.809)	-1.6 (-1.4)	-112.1 (-111.4)
	2.605 (2.616)	2.684 (2.704)	1.781 (1.767)	-1.6 (-1.5)	-112.5 (-111.7)
	(2.788)	(2.893)	(1.752)	(-1.6)	(-111.8)
[CO_2^-]	1.967	1.992	1.829	1.2	-105.4
C3-down[b]	2.273 (2.250)	2.317 (2.305)	1.862 (1.858)	1.9 (1.9)	-108.3 (-107.7)
	2.604 (2.614)	2.683 (2.701)	1.827 (1.813)	2.0 (2.0)	-108.8 (-108.3)
	(2.788)	(2.888)	(1.797)	(2.1)	(-108.2)
[CO_2^-]	1.973	1.980		-2.7	53.9
N-up[b]	2.276 (2.256)	2.306 (2.289)		-1.0 (-1.5)	52.7 (52.9)
	2.608 (2.619)	2.664 (2.679)		-2.2 (-2.4)	52.7 (52.8)
	(2.794)	(2.862)		(-2.6)	(52.9)
[CO_2^-]	1.959	1.990		9.9	-53.2
C1-up[b]	2.240 (2.244)	2.287 (2.299)		8.4 (9.1)	-52.3 (-51.2)
	2.596 (2.608)	2.676 (2.692)		8.3 (8.8)	-51.7 (-51.4)
	2.779	(2.881)		(8.6)	(-51.4)
[COOH]	[CO_2^-] C3-up	[CO_2^-] C3-up	[CO_2^-] C3-up	[CO_2^-] C3-up	[CO_2^-] C3-up
C3-up[c]	2.276 ([CO_2^-] C3-up)	2.429 ([CO_2^-] C3-up)	1.614 ([CO_2^-] C3-up)	1.0 ([CO_2^-] C3-up)	-107.6 ([CO_2^-] C3-up)
	2.621 (2.631)	2.874 (2.898)	1.708 (1.693)	1.2 (1.2)	-105.9 (-105.3)
	(2.804)	(3.137)	1.720	(1.2)	(-104.8)
[COOH]	[CO_2^-] C3-down	[CO_2^-] C3-down	[CO_2^-] C3-down	[CO_2^-] C3-down	[CO_2^-] C3-down
C3-down[c]	2.280 ([CO_2^-]C3-down)	2.420 ([CO_2^-]C3-down)	1.615 ([CO_2^-]C3-down)	2.4 ([CO_2^-]C3-down)	-108.9 ([CO_2^-]C3-down)
	2.621 (2.632)	2.871 (2.897)	1.721 (1.713)	3.0 (3.1)	-105.3 (-105.3)
	(2.807)	(3.133)	(1.745)	(3.3)	(-101.7)
[COOH]	1.997	2.099	1.923	-8.5	67.1
N-up[c]	2.284 (2.255)	2.462 (2.509)	2.117 (2.128)	-6.9 (-6.9)	63.2 (62.5)
	2.628 (2.633)	2.958 (3.023)	2.135 (2.146)	-6.8 (-6.7)	62.2 (61.5)
	(2.804)	(3.306)	(2.149)	(-6.6)	(61.3)

Species	r(M^+— O) (Å)	r(M^+— X) (Å)	hydrogen bond (Å)	∠HOCC (deg)	∠CCNC (deg)
[N,CO]	1.890	2.062	2.305	176.6	-95.6
C4-down,	2.227 (2.213)	2.450 (2.454)	2.320 (2.318)	176.5 (176.5)	-87.8 (-87.0)
t[d]	2.577 (2.590)	2.889 (2.929)	2.319 (2.315)	176.4 (176.5)	-81.7 (-81.4)
	(2.765)	(3.161)	(2.314)	(176.6)	(-80.9)
[N,CO]	1.927	2.072		2.9	65.4
C4-down,	2.253 (2.236)	2.453 (2.459)		4.3 (4.2)	61.4 (61.1)
c[d]	2.592 (2.604)	2.911 (2.940)		4.6 (4.5)	59.6 (59.1)
	2.777	3.173		(4.7)	(58.5)
[N,CO]	1.946	2.056	2.317	-176.0	65.5
N-up, t[d]	2.279 (2.263)	2.422 (2.425)	2.324 (2.321)	-175.7 (-175.7)	61.4 (61.4)
	2.629 (2.639)	2.853 (2.883)	2.318 (2.313)	-175.8 (-175.8)	59.5 (59.2)
	(2.823)	(3.092)	2.311	(-175.8)	(58.6)
[N,OH]	1.895	2.031	2.312	-174.6	-82.8
N-up[d]	2.278 (2.276)	2.393 (2.392)	2.283 (2.274)	-175.4 (-175.4)	-77.5 (-77.5)
	2.672 (2.698)	2.804 (2.833)	2.264 (2.255)	-175.5 (-175.8)	-75.7 (-74.8)
	(2.893)	(3.042)	(2.250)	(-175.9)	(-74.1)
[CO]	[N, CO] C4-down, t		[N, CO] C4-down, t	[N, CO] C4-down, t	[N, CO] C4-down, t
C1-up, t[e]	2.159 (2.150)		2.315 (2.315)	178.2 (178.2)	61.9 (-62.8)
	2.510 (2.529)		2.317 (2.315)	177.8 (177.9)	-59.9 (-60.2)
	(2.713)		(2.315)	(177.8)	(-59.8)
[CO]	1.810			-2.2	-56.6
C1-up, c	2.153 (2.139)			-1.4 (-1.5)	-57.2 (-57.7)
	2.524 (2.543)			-1.8 (-1.6)	-57.3 (-57.6)
	(2.726)			(-1.9)	(-57.7)

[a]Geometries calculated at the MP2(full)/cc-pVDZ(Li-C) level for Li^+(NMP); at the B3LYP/6-311+G(d,p) and B3LYP/def2-TZVP (in parenthesis) levels for Na^+(NMP), K^+(NMP), Rb^+(NMP), listed in the order Li^+(NMP) (top) - Rb^+(NMP) (bottom). [b] X = O. Hydrogen bond = r(NH···OC). [c] X = OH. Hydrogen bond = r(N···HO). [d] X = N. Hydrogen bond = r(CO···HO). [e] Hydrogen bond = r(CO···HO).